PNAS RESEARCH ARTICLE | ENGINEERING ENVIRONMENTAL SCIENCES

Climate change impacts on tropical cyclone–induced power outage risk: Sociodemographic differences in outage burdens

Seth Guikema[a,b,1], Zaira Pagan-Cajigas[b], Charles Fant[c], Brent Boehlert[c], C. X. Maier[c], Kerry Emanuel[d], Corinne Hartin[e], and Marcus C. Sarofim[e]

Affiliations are included on p. 9.

Edited by Dennis Hartmann, University of Washington, Seattle, WA; received March 5, 2025; accepted August 11, 2025

This research investigates the projected risks of future climate trends on tropical cyclone–induced power outages in the Gulf and Atlantic coast of the United States, focusing on the disproportionate impacts on vulnerable populations and the economic burdens associated with such events. Our methodology integrates four well-documented models to estimate changes in power outage rates, sociodemographic inequities, and economic costs due to tropical cyclone projections. Synthetic tropical cyclones were generated using data from seven global climate models (GCMs), used to compare power outage risks at the census tract level along two periods: hindcast (1995–2014) and late-century (2071–2100) using the SSP5-8.5 scenario. The late-century results from each model were scaled to align with a global warming scenario of 3 °C. We evaluated the uncertainty of these projections by considering the agreement among the GCMs outage projections. Results highlight a significant increase in power outage risks and high agreement in northern Florida, Georgia, the mid-Atlantic, and the North Atlantic coast. Distributional impact analyses indicate higher outage risks for Hispanic, non-White, and low-income populations, while economic projections show annual costs rising from $6.2 billion in the hindcast to over $11 billion for the 3 °C scenario. The findings highlight the need for adaptive strategies and equitable resource allocation to mitigate these growing risks due to future climate projections.

electric system reliability | climate change | power outages | tropical cyclones | interruption cost

Significance

This study integrates advanced modeling approaches to project risks of tropical cyclone–induced power outages under changing climate conditions. Combining climate simulations, machine learning, distributional impact, and economic analyses, this research identifies regions and vulnerable populations along the US Gulf and Atlantic coasts that are disproportionately affected by these outages. These insights emphasize the urgent need for adaptive planning, equitable resource allocation, and targeted mitigation strategies to address the growing societal and economic impacts of climate-driven outages.

Weather events are the primary cause of power outages in the United States, accounting for 78% of major disruptions (1). The impact of these weather-induced outages has increased substantially over the past two decades (2) and is expected to further rise as the changing climate intensifies extreme weather events. These outages have far-reaching implications, disproportionately affecting vulnerable populations who face significant social and economic burdens, such as disrupted access to critical services, health risks from power-dependent medical devices, and income losses (3).

Evidence indicates that lower-income communities experience longer restoration times, exacerbating existing disparities in health, safety, and overall well-being (4). In addition to their societal impacts, these outages also place a significant economic burden (5). Annual costs of weather-related power outages in the United States are currently estimated to range from $25 billion to $400 billion, with projections suggesting further increases as extreme weather events become more frequent and severe (5–7).

Tropical cyclones in particular are responsible for 9 out of 10 major outages in the United States (8). Recent studies show that tropical cyclones are intensifying more rapidly, producing more rainfall, moving more slowly, extending further inland, and causing increased storm surges (9). These trends are consistent with research correlating a warming climate to shifts in tropical cyclones' behavior, such as increased maximum surface wind speeds, poleward shifts of storm tracks, increased precipitation, slower translation speed, and a global increase in the frequency of high-intensity cyclones (10).

Over the next century, warming sea surface temperatures and changes in atmospheric conditions may further alter the cyclonic behavior, potentially changing their frequency, wind speed, and size. Along the US Gulf and Atlantic coasts, medium-confidence projections suggest further increases in cyclone intensity, wind speeds, precipitation, storm surge, and intensification rates (11). However, it remains uncertain which regions and demographic groups in the United States may face disproportionately higher impacts from these outages as climate conditions continue to shift. Proactive planning for these changes enables decision-makers to prepare for variations in the occurrence of major power interruptions.

Author contributions: S.G., Z.P.-C., C.F., B.B., C.H., and M.C.S. designed research; Z.P.-C., B.B., C.X.M., and K.E. performed research; S.G. and Z.P.-C. contributed new reagents/analytic tools; S.G., Z.P.-C., C.F., and B.B. analyzed data; K.E. reviewed and edited paper; and S.G., Z.P.-C., C.F., B.B., C.X.M., C.H., and M.C.S. wrote the paper.

Competing interest statement: S.G. is with the University of Michigan. Z.P.-C. is with the University of Michigan C.F. is with Industrial Economics, Inc. B.B. is with Industrial Economics, Inc. C.X.M. is with Industrial Economics, Inc. K.E. is with WindRisk, LLC and serves on the Boards of Directors of Trusted Underwriting and Plymouth Rock Home. His research on this topic is supported by the Eric and Wendy Schmidt Foundation and by the MIT Climate Grand Challenges program. C.H. is with the US EPA M.C.S. is with the US EPA. S.G. has stock ownership in One Concern, Inc., a company working in the broader climate resilience space. However, they did not fund this work and do not have a direct interest in the work in this paper. K. Emanuel's research is part of the MIT Climate Grand Challenge on Weather and Climate Extremes. Support was provided by Schmidt Sciences, LLC.

This article is a PNAS Direct Submission.

[1]To whom correspondence may be addressed. Email: sguikema@umich.edu.

This article contains supporting information online at https://www.pnas.org/lookup/suppl/doi:10.1073/pnas.2502266122/-/DCSupplemental.

Published October 13, 2025.

Many models have been developed to estimate power outages due to tropical cyclones, ranging from detailed parametric and semiparametric statistical models (e.g., 12, 13) to advance machine learning models (e.g., 14–19). Particularly relevant to this study are models that use a reduced set of variables available at fine spatial scales (e.g., 14) or those which rely only on publicly available data, thereby avoiding dependence on utility-specific data, which is often restricted or unavailable (e.g., 20).

Previous modeling efforts have identified key predictors of power outages, including gust wind speed, duration of winds exceeding 20 m/s, land use, and population density (14, 20). These predictors are crucial for improving model accuracy and understanding the factors driving outage patterns. In contrast, other factors such as storm surges are generally not significant predictors of power outages beyond a narrow coastal strip (21, 22).

Additional analysis of outage characteristics suggests that areas managed by rural utilities experience longer restoration times compared to urban regions (23). Similarly, wealthier areas tend to have power restored faster than less affluent ones, even when accounting for storm strength and initial impact (4). These disparities disproportionately affect vulnerable communities, including low-income households, the elderly, and non-Hispanic Black and Hispanic populations, who are less likely to have access to backup power solutions (24) and often endure prolonged outages (25, 26).

These power outages also have broader economic implications. Understanding the economic implications of cyclone-induced outages is essential for decision-makers, as it provides a basis for comparing sectoral impacts and evaluating adaptation strategies, thereby guiding effective resource allocation. A commonly used metric to estimate these impacts is the Customer Interruption Cost (CIC), also known as the Value of Lost Load. CIC can be estimated using various methods, including survey-based stated preferences, market-based revealed preferences, and regional economic modeling (27).

To make these CIC insights more accessible, the US Department of Energy, in collaboration with Lawrence Berkeley National Laboratory and Resource Innovations, Inc., developed the Interruption Cost Estimate (ICE) Calculator. This online tool consolidates the results of many existing CIC studies, offering utilities and other stakeholders a practical resource for estimating the economic costs of power interruptions for residential, commercial, and industrial customers (27). The ICE Calculator is based on a meta-database of 34 existing CIC studies, containing more than 100,000 survey responses. This tool incorporates relevant regional data such as annual power usage, household income, timing of outages, and commercial and industrial customer characteristics, allowing for customization in each analysis (27, 28).

To improve our understanding of climate change's impact on electric power outages, individuals, and the US economy, this paper estimated changes in 1) power outage rates, 2) inequities in power outage rates, and 3) the costs of power interruptions, all associated with landfalling tropical cyclones in the Gulf and Atlantic Coasts of the United States. Our approach integrates four models: a Tropical Cyclone Simulator Model, a Power Outage Prediction Model, an Distributional Impact Model, and an Economic Model.

This analysis begins with the Tropical Cyclone Simulator Model, which uses a dynamic downscaling technique to generate tropical cyclone tracks from seven coarse-resolution global climate models (GCMs). Tracks are produced for both a hindcast period (1985–2014) and a late-century period (2071–2100) under a high emissions scenario, namely SSP5-8.5. This scenario is projected to lead to a global temperature increase of approximately 2.9 to 5.6 °C by the late century. This scenario is not a likely outcome of current emissions but is useful for generating damage functions that can be expressed in terms of by-degree warming (29). The results of the study are then scaled to 3 °C of warming globally, similar to the 2.8 °C that Sarofim et al. (29) estimate is the median future warming scenario.

The simulated tropical cyclone tracks are used to estimate surface wind speeds for 45,707 census tracts along the Gulf and Atlantic Coasts of the United States for each of the generated tropical cyclones. These near-surface wind statistics serve as input to the second model, the Power Outage Prediction Model, a machine learning model trained on past tropical cyclone events to estimate the fraction of customers who experience power outages in each census tract for each tropical cyclone event.

The fraction of customers who experience power outages serves as the response variable in the Distributional Impact Model, which uses a random forest regression model to evaluate the projected impacts of these outages on diverse sociodemographic and socioeconomic groups. This analysis provides insights into the potential burdens on vulnerable populations. Finally, the Economic Model estimates the customer interruption cost by integrating the outputs of the ICE Calculator with typical cyclone power restoration times based on historical events in the United States

Each of these individual models is well documented in the literature. The contribution of this paper is not in advancing any single model, but rather in integrating them to offer insights into potential future increases in impacts from tropical cyclone–induced power outages. The insights gained not only highlight the regions and populations at greatest risk but also provide actionable information for policymakers, utility companies, and emergency planners to develop more targeted mitigation and adaptation strategies.

1. Results

1.1. Changes in Tropical Cyclone Hazard and Power Outage Frequency. Fig. 1 shows the projected changes in the annual frequency of tropical cyclones by Saffir–Simpson category classification, based on the maximum wind speed at first U.S. landfall. Five out of seven GCMs project an overall increase in the frequency of tropical cyclones by the end of the century. However, these increases are not uniformly distributed across the cyclone categories. Specifically, five of the seven GCMs project a decrease in the frequency of tropical storms, compared to their respective hindcast, while all seven GCMs project an increase in Category 5 hurricanes. These findings indicate that overall, tropical cyclones are likely to be more intense and damaging by the late century, generally in agreement with the existing literature (e.g., 30).

Fig. 2 shows the projected changes in the annual proportion of the population experiencing power outages per census tract, calculated as the difference in power outage rates between the hindcast period (1995–2014) and the late century period (2071–2100), considering a 3 °C warming scenario. The map highlights the magnitude of change in outage rates and the level of agreement among climate models.

The most significant increases in outage rates are expected in northern Florida and Georgia, regions currently experiencing moderate outage risks (*SI Appendix*, Fig. S6) but projected to face substantial increases by the late century. Expected increases in outage rates extend northward, reaching as far as the New England coast. This includes areas with historically low outage risks, which are now projected to experience significant increases in the frequency and duration of power outages.

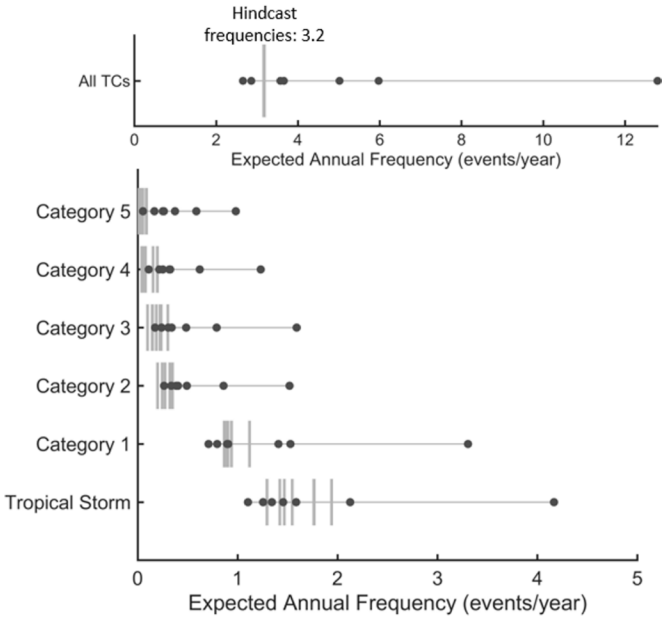

Fig. 1. Annual frequency of all tropical cyclones (TCs) included in the analysis (*Upper* panel) and the annual frequency of tropical cyclones by the Saffir–Simpson scale (*Lower* panel). The gray solid vertical lines show the GCM hindcasts representing 1985–2014, where each vertical line represents a GCM. The projected frequency for each of the seven GCMs at 3° is represented by dots.

Northern Florida, Georgia, the mid-Atlantic, and North Atlantic coasts emerge as areas of high concern, showing both significant increases in outage rates and strong agreement among models. In contrast, areas like the Gulf Coast exhibit low GCM agreement, indicating substantial uncertainty in the direction and magnitude of projected outage changes. These findings point to the dual need for robust climate adaptation strategies in regions with high agreement and significant outage risks, as well as further research to better understand and reduce uncertainties in low-agreement regions. Additional information on model-by-model outage projections is included in the Supporting Information.

Fig. 3 displays the total household outage hours across multiple tropical cyclone return periods (2, 5, 20, and 100 y), broken down by region. The results indicate that the range of estimated outage hours increases at higher return period events across all regions. Notably, at the 100-y return period level, the North Atlantic region experiences the highest outage hours, driven partly due to its larger population compared to other regions. Only high-intensity tropical cyclones impacting this region are likely to produce outages at the upper end of the outage-hour range.

Taken together, the outage results suggest substantial increases in tropical cyclone–induced outages in northern Florida and Georgia, and along the mid-Atlantic and North Atlantic coasts. Beyond these areas, there is higher uncertainty about both the magnitude and direction of future changes. However, all models suggest that the more extreme tropical cyclone events will result in increased outage hours across all four regions evaluated.

1.2. Inequality of Impacts Across Subpopulations. To investigate differences in outage rates across subpopulations, we trained a Random Forest model using the census tract outage rate as the response variable and sociodemographic variables as the explanatory features. Following the method of Shortridge and Guikema (31), we calculated the total change in the marginal effect of each sociodemographic variable on the outage rate from its partial dependence plot. This metric, referred to as the "swing", captures the range between the minimum and maximum predicted values for each variable while holding other factors constant. A positive swing indicates that census tracts with higher values for a given sociodemographic group are associated with higher outage rates in the margin.

In addition to individual sociodemographic variables, the Social Vulnerability Index (SVI) was included in the analysis to assess the extent to which census tracts with a high SVI align with those identified as most at risk for power outages. The SVI is a composite measure that incorporates multiple factors contributing to vulnerability, including socioeconomic status, household composition, disability, minority status, and language proficiency, as well as housing and transportation accessibility.

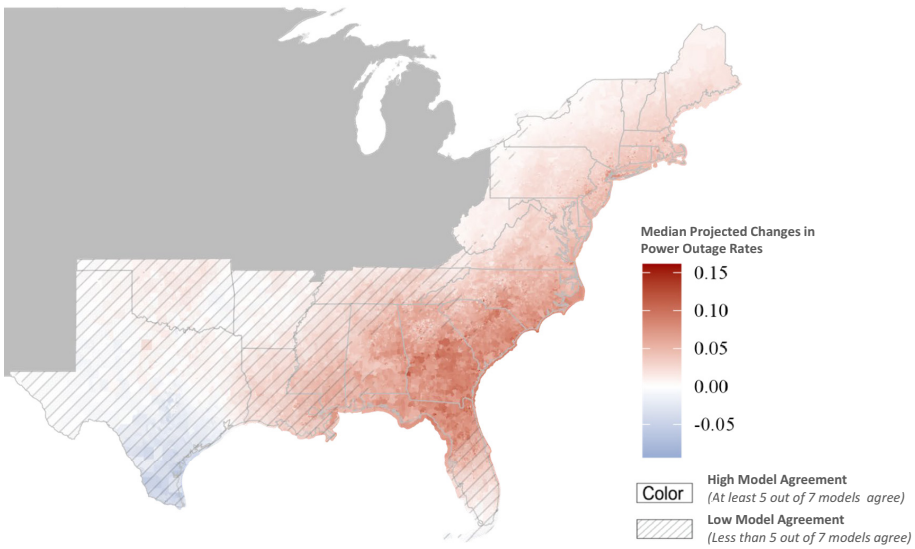

Fig. 2. Projected changes in the annual proportion of the population experiencing power outages per census tract, calculated as the difference in power outage rates between the hindcast period (1995–2014) and the late century period (2071–2100) considering a 3 °C of warming scenario. Colors indicate the magnitude of change in outage rates, with red areas suggesting an increased risk of power outages. Regions with high model agreement, where at least 5 out of 7 models concur on the direction of change, are shaded solid. In contrast, regions with low model agreement, where fewer than 5 models align, are marked with diagonal stripes, highlighting areas of greater uncertainty in the projected direction of change.

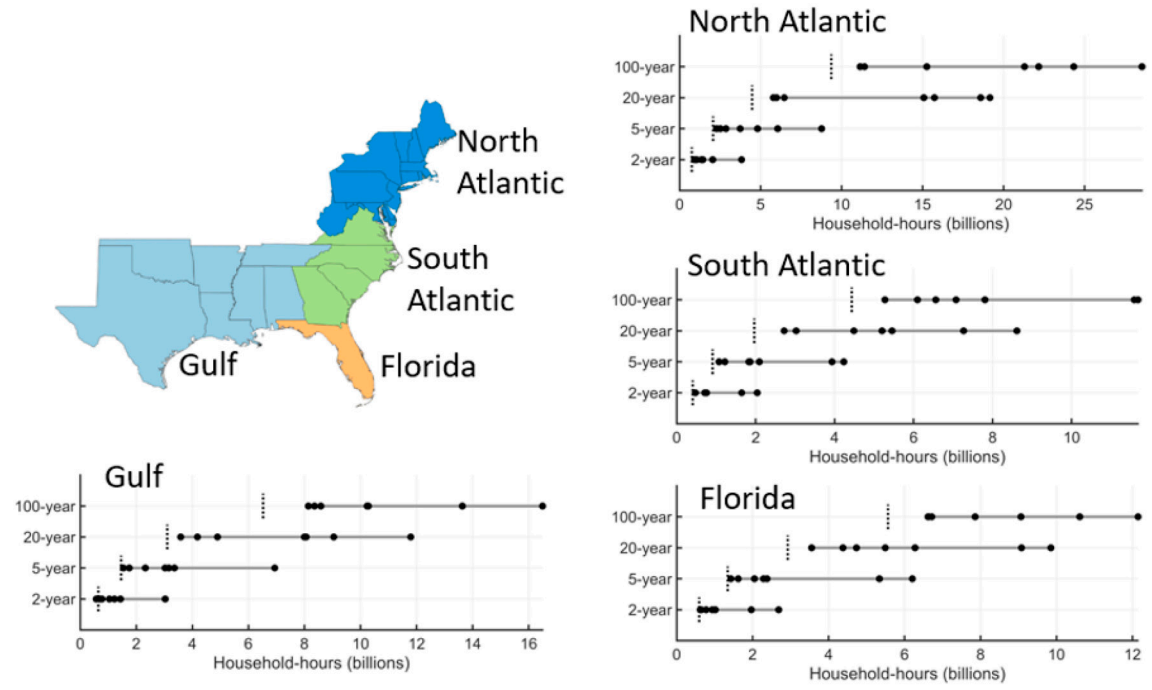

Fig. 3. Projected residential household hours without power for 100-y, 20-y, 5-y, and 2-y tropical cyclone events, categorized by region. Each dot represents one of the seven GCMs under the 3 °C warming scenario. The dashed vertical black line indicates the hindcast mean. For this figure, household hours for each GCM are calculated as the difference between the GCM-specific hindcast and projection, added to the hindcast mean (shown by the dashed vertical line).

To account for geographic variability in tropical cyclone exposure and population characteristics, this analysis was conducted across four distinct regions of the United States: North Atlantic, South Atlantic, Gulf, and Florida. Fig. 4 presents swing values for eight sociodemographic variables across both historical (hindcast) and future climate scenarios (3 °C warming) scenarios, disaggregated by region. Across regions, census tracts with higher proportions of non-White and Hispanic populations consistently exhibit higher outage risks. These groups frequently show the largest positive swing values, indicating persistent vulnerability to tropical

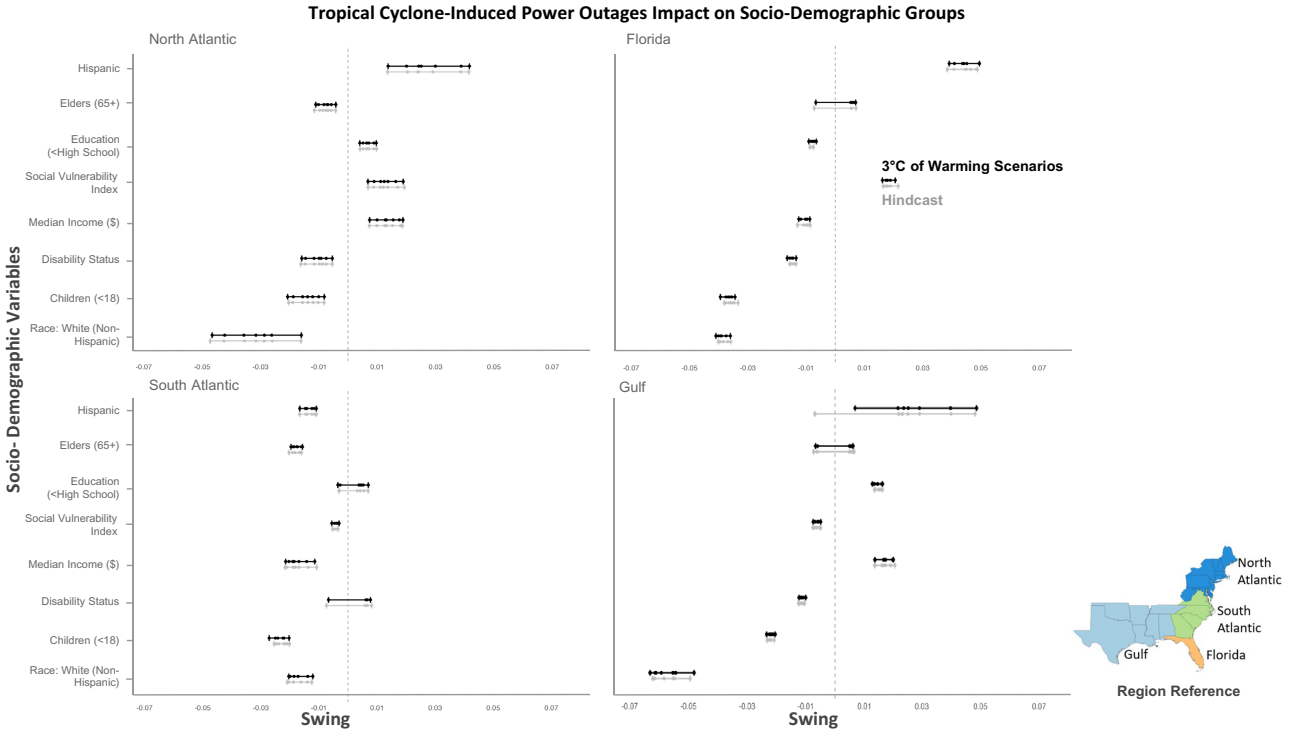

Fig. 4. Swing estimates per sociodemographic group for the Hindcast and the 3 °C warming scenario per region. Each dot represents one of the seven GCMs. The swing measures the marginal effect of a sociodemographic variable on power outage rates, as calculated using partial dependence plots. A positive swing indicates that census tracts with higher current concentrations of the specified sociodemographic group experience a larger marginal increase in the frequency of power outages, with larger values reflecting a stronger effect. Conversely, a negative swing suggests that census tracks with a higher representation of the group have a negative marginal effect in outages compared to others.

Table 1. Economic impacts by customer type, showing total annual costs and per-customer costs under the hindcast scenarios, along with the additional costs (in italic) projected for the 3 °C warming scenario

Customer type	Annual cost ($bill, Hindcast)	Additional annual cost ($bill, 3 °C of warming)	Annual cost per customer (Hindcast)	Additional annual cost per customer (3 °C of warming)
Residential	**$0.12** ($0.11 to $0.15)	+$0.10 (−$0.01 to $0.41)	**$1.9** ($1.6 to $2.3)	+$1.6 (−$0.1 to $6.4)
Small commercial and industrial	**$3.42** ($2.82 to $4.31)	+$3.00 (−$0.19 to $11.95)	**$431** ($355 to $544)	+$379 (−$24 to $1,505)
Medium/large commercial and industrial	**$2.67** ($2.21 to $3.08)	+$1.98 (−$0.24 to $8.26)	**$2,477** ($2,052 to $2,853)	+$1,839 (−$219 to $7,657)
Total	**$6.22** ($5.14 to $7.54)	+$5.09 (−$0.44 to $20.62)		

The first value in each cell represents the mean (in bold) across all GCMs, with the minimum and maximum estimates from the GCMs in parentheses. All values are in 2020 dollars.

cyclone–induced power outages under both current and future climate conditions.

At the region level, individual swing directionality and magnitude differ. In the North Atlantic region census tracts with higher concentrations of Hispanic and non-White populations, individuals with less than a high school education, higher SVI scores, and higher median incomes, are more likely to experience significant impacts both now and in the future. This suggests that future risk in this region may increasingly affect both traditionally vulnerable groups and some higher-income areas.

In Florida, higher outage risks are associated with tracts that have larger proportions of Hispanic populations, elderly individuals (65+), and high SVI scores. These findings highlight a persistent concentration of outage vulnerability among older and socially vulnerable populations in the state. For the South Atlantic region, the swing effect for non-White populations is smaller compared to other regions. Instead, outage risk is more strongly associated with lower educational attainment and higher disability prevalence, suggesting different underlying vulnerability structures.

Finally, the Gulf region swing results indicate census tracts with larger proportions of Hispanic and non-White residents, elderly populations, population with education below high school, and, similar to the North Atlantic, higher median household income have higher outage risk due to tropical cyclones. While the general direction of swing values remains stable over time, these regional differences suggest that climate-driven changes in tropical cyclone behavior may interact with existing social patterns in complex ways. The consistency of high swing values between hindcast and projected conditions for certain populations underscores persistent structural vulnerabilities, while shifts in other variables (e.g., income or disability) may reflect spatial changes in storm impacts under future climate scenarios.

1.3. Economic Impact Results. Table 1 summarizes the annual economic impacts of power outages from tropical cyclones, as estimated by ICE, with both total cost and cost per customer shown. The hindcast mean cost of $6.2 billion annually is expected to increase to approximately $11 billion on average under the 3 °C warming scenario. Results vary widely across GCMs, ranging from $5.4 billion to $26 billion annually. Looking at per-customer costs, the medium and large commercial and industrial customers bear the bulk of the outage burden in economic terms, even though residential customers account for 88% of all customers in the domain. Projecting the number of customers for the late century, using population projections for residential customers and expected trends for commercial and industrial customers, results in $20 billion annually with 3 °C warming, ranging from $9.5 to $47 billion across GCMs (see Supporting Information for population projections).

2. Discussion

This study highlights the growing risks of tropical cyclone–induced power outages in the United States based on 3 °C of warming. Our analysis reveals substantial increases in both the frequency and intensity of tropical cyclones, leading to longer outage durations, particularly in the Gulf, Atlantic, and Northeastern regions. Importantly, all GCMs evaluated project that power outage impact will extend further inland under future climate conditions, with significant increases along the northern region of the Atlantic coast—a region historically less vulnerable to such disruptions. This shift highlights the need for utilities and policymakers to address evolving risks in previously low-exposure areas.

The analysis of inequalities in impacts across subpopulations highlights disproportionate impacts on vulnerable populations, including census tracts with high concentrations of Hispanic populations, low-income households, and elderly residents. Simultaneously, the economic burden of these outages is projected to nearly double, rising from $6.2 billion to over $11 billion annually based on the 3 °C warming scenario. Medium and large commercial and industrial customers are expected to bear the highest per-customer costs, reflecting their reliance on reliable electricity.

Despite these challenges, utilities have opportunities to mitigate risks through adaptive measures. Establishing strategies such as routine maintenance, undergrounding power lines, and asset hardening can significantly reduce the likelihood of outages. Additionally, innovations like smart grid technologies and optimized restoration responses offer opportunities to enhance resilience. However, the widespread implementation of these measures requires substantial financial and operational investments, and many utilities remain constrained by limited budgets and resources.

The reliance on seven GCMs and the SSP5-8.5 high-emissions scenario provides a robust framework for projecting outage risk under a warming scenario. However, the scaling to 3 °C of warming assumes linearity in impacts—explicitly calculating those changes using a different SSP scenario could result in different projections of tropical cyclone frequency, intensity, and associated power outages. Expanding the analysis to include a broader ensemble of GCMs and additional emissions pathways would enhance our understanding of uncertainties and provide a more comprehensive view of potential future outcomes.

The power outage model used in this study, while robust, has several limitations that could influence its predictive accuracy. For instance, the exclusion of critical covariates such as tree characteristics—due to their unavailability at a multistate scale—may reduce the model's ability to capture vegetation-driven outage risks. Additionally, the model's training relies on historical outage

data (1985–2014), which may not fully account for future changes in grid infrastructure, urbanization, or adaptive measures.

Furthermore, the power restoration model used in our analysis is a simplified representation that assigns a uniform outage duration to all impacted areas for a given event. This approach, while enabling streamlined integration into the economic model, misestimates spatial patterns of outages, likely underestimating durations near the landfall locations and overestimating durations in inland areas. It also neglects key factors that influence variability, such as utility-specific crew management practices, real-time operational decisions, and localized challenges in infrastructure recovery. Future work will address these limitations by incorporating more robust restoration models that account for spatial and operational variability in restoration processes.

Similarly, the ICE Calculator, used to estimate economic impacts, is constrained by its reliance on customer interruption cost (CIC) data, which is geographically uneven and significantly underrepresents the northeastern United States. Additionally, the calculator may not fully capture the broader economic effects of prolonged outages. While its results offer valuable insights, they remain constrained by the underlying CIC dataset, based on studies conducted between 1989 and 2012, and the econometric model, which was last refined in 2018. Enhancing these datasets and models in the future could substantially improve the accuracy and relevance of our model in estimating outage costs.

Beyond the direct impacts of tropical cyclones, climate change introduces additional vulnerabilities to the grid. Changes in vegetation growth, tree stability, and infrastructure degradation—such as power pole degradation—pose further risks to grid reliability (32). While these were not included in our current model, incorporating these factors into future models could improve the accuracy and utility of outage projections. Furthermore, it is worth acknowledging that advances in grid design, such as increased undergrounding of power lines, the deployment of smart grid technologies, microgrids, and improved storm forecasting and outage response systems, may significantly enhance grid resilience by 2100. While these developments are difficult to predict and were beyond the scope of this analysis, they could mitigate some of the projected risks.

This study provides a significant contribution to understanding the risks associated with future climate scenarios. By integrating physical, economic, and sociodemographic analyses at the census tract level, this study offers a robust framework to inform policy and investment decisions. These insights aim to enhance grid resilience and mitigate the societal impacts of future power outages. Our findings highlight the need for proactive adaptation strategies, equitable resource allocation, and ongoing research to address the uncertainties and vulnerabilities associated with a changing climate.

3. Methods

This approach utilizes four established model frameworks–the Tropical Cyclone Simulator Model, Power Outage Prediction Model, Distributional Impact Model, and the Economic Model–to improve our understanding of climate change's impact on power outages, individuals, and the US economy. The Tropical Cyclone Simulator Model generates synthetic tropical cyclone storm tracks using atmospheric data from GCMs. These storm tracks are then used in the Power Outage Prediction Model, which estimates the fraction of customers experiencing power loss in each event, analyzed at the US Census tract level. To further assess the social implications, the outage results were used as inputs for the Distributional Impact Model, which uses a random forest regression model to evaluate how projected outages might affect various sociodemographic subgroups. The Economic Model subsequently calculates the economic impact of these power interruptions. The methodology for these integrated frameworks is shown in Fig. 5.

3.1. Tropical Cyclone Simulation Model.

3.1.1. Synthetic tropical cyclone generator. We employ a well-established dynamic downscaling technique that simulates ensembles of tropical cyclone tracks from coarse-resolution GCMs. The approach, described in detail by Emanuel et al. (33, 34) with updates by Emanuel (35) and Komurcu et al. (36), uses monthly sea surface temperature, atmospheric temperature, humidity, and daily horizontal wind speeds to generate proto-vortices. These weak proto-vortices are used to initialize the intensity model.

Storm intensity is driven by a coupled ocean-atmosphere, quasi-balanced, axisymmetric numerical model. Most initial proto-vortices, or "seeds", are discarded as they fail to meet an intensity threshold of 7 m/s within two days or a lifetime maximum wind speed of 20.58 m/s (40 kn). This filtering process ensures that only storms forming under suitable thermodynamic and kinematic conditions are included in the ensemble, resembling a natural selection process. For each year, the model generates synthetic storms until an established number of successful storms is achieved, recording both the successful and unsuccessful attempts.

To ensure consistency across models, simulations for the hindcast period (1985–2014) are calibrated to have the same average storm frequency. This calibration is achieved by applying a proportionality constant to the ratio of successful to unsuccessful seeds, which serves as the basis for estimating annual storm frequencies and aligning them with historical observations from the ERA5 reanalysis dataset (37).

The calibrated proportionality constants derived from the hindcast period are then applied to late-century simulations, which for this analysis are based on the SSP5-8.5 scenario. These parameters remain constant for future simulations, allowing the model to naturally produce variations in tropical cyclone frequency and intensity due to changes in climate conditions. The simulated changes in tropical cyclone frequency are due to variations in the survival rate of seeds, driven by shifts in climate drivers such as sea surface temperatures (SST), atmospheric temperatures, and humidity. This approach ensures that the simulations reflect the influence of a warming climate on tropical cyclone genesis and intensification.

The projected changes in storm frequency vary across models. While some of this variability is due to differing climate sensitivities, scaling to 3 °C of warming helps account for these differences. Variations in sea surface temperature patterns, wind shear, and other parameters further contribute to differences among GCMs. This variability highlights the importance of an ensemble approach, which captures a broader range of possible outcomes and provides a more robust understanding of how tropical cyclone frequencies may evolve under future climate conditions.

The modeled frequency and power dissipation from the hindcasts are used to select a set of seven CMIP-6 GCMs: EC-Earth3, MRI-ESM2-0, MPI-ESM1-2-HR, UKESM1-0-LL, CESM2, MIROC6, and CNRM-CM6-1. Additional details on this GCM selection process are provided in the Supporting Information (Section 1). Using this method, we generate 2,000 tropical cyclone tracks and intensities for each GCM hindcast period (1985–2014) and an additional 2,000 tracks and intensities for a late-century period (2071–2100) under the SSP5-8.5 high emissions scenario. The application of SSP5-8.5 in this analysis is not a judgment regarding the likelihood of that scenario. Its use here is relevant and useful in that it encompasses the broadest range of possible future temperatures, including higher warming levels, and there is higher confidence in interpolation between temperature data points than in extrapolation beyond those points (38, 39).

3.1.2. Estimates of impacts by-degree. Results are presented for a global warming scenario of 3 °C. To estimate these results, we scale the data using the ratio of 3 °C to the global temperature change from the GCM hindcast to the late-century period. This approach ensures comparability across models and scenarios, allowing the analysis to focus on outcomes under a uniform 3 °C warming scenario while accounting for the inherent differences in model predictions. Additional details, including global temperature changes by GCM, are provided in the Supporting Information (*SI Appendix*, Table S3).

3.1.3. Parametric wind field model. To estimate local wind speed statistics for each census tract, we used a parametric wind field model based on the Willoughby et al. (40), publicly available through the R package "stormwindmodel." This model has been applied in previous studies by Han et al. (12), and Tonn et al. (22). It calculates surface-level sustained winds, 3-s wind gusts, and the duration of winds exceeding a specified threshold at the centroid of

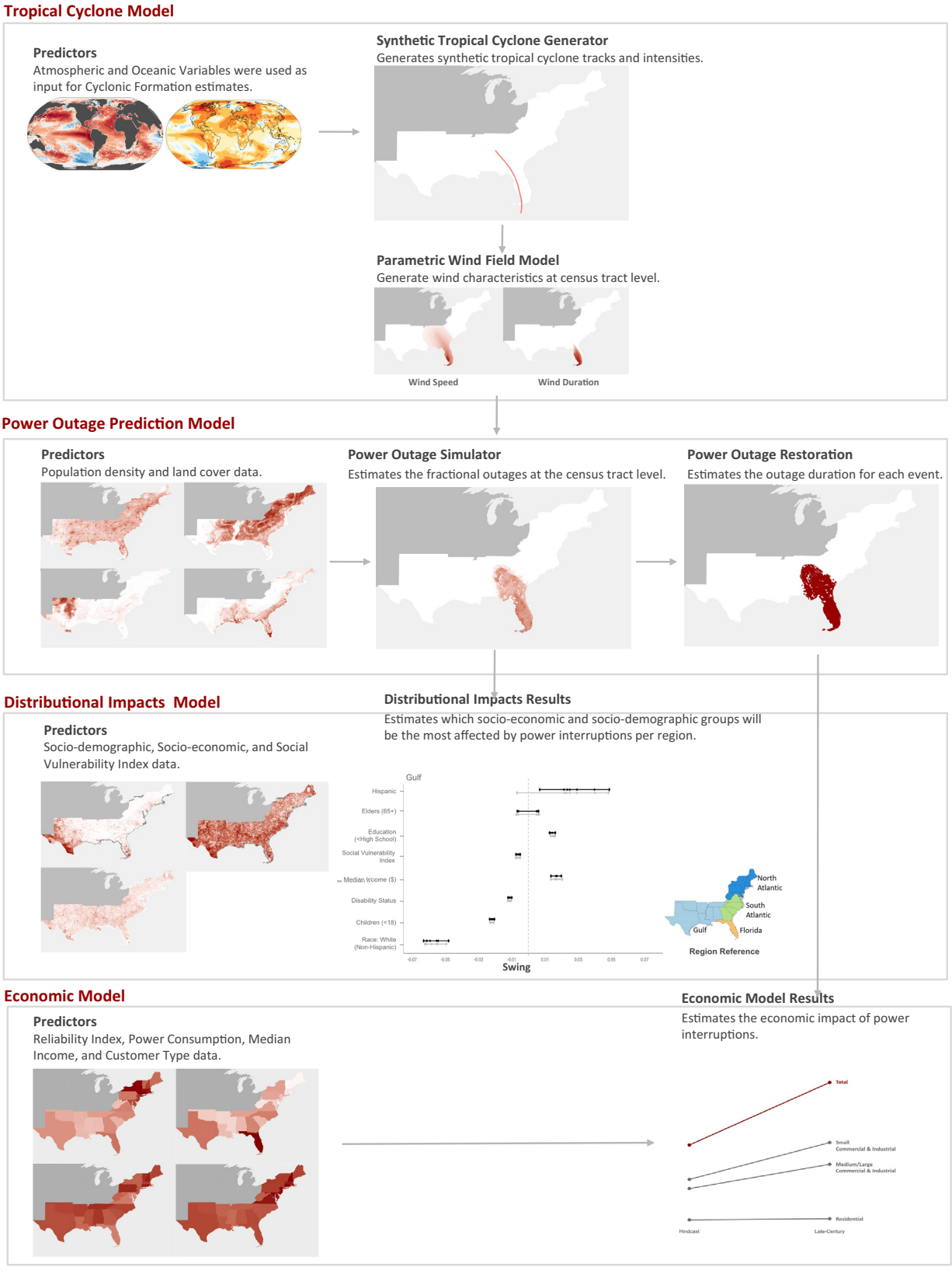

Fig. 5. Overview of methodology for estimating the economic and social impact associated with tropical cyclone–induced power outages.

each census tract based on the tropical cyclone's location and maximum wind speed recorded at 2-h intervals from the Synthetic Tropical Cyclone Generator Model. For our analysis, we set the cutoff wind speed at 20 m/s, following the methodology of Han et al. (12). The model outputs–maximum gust wind speed at the surface level and the duration of sustained winds exceeding 20 m/s–are incorporated as input parameters in the Power Outage Prediction Model. Additional details on the Parametric Wind Field Model are provided in the Supporting Information.

3.2. Power Outage Prediction Model.

3.2.1. Parameter selection. We utilized an outage model adapted from Guikema et al. (20) and McRoberts et al. (41) to estimate the fraction of the customers in each census tract that will experience power outages during a tropical cyclone. An earlier model developed by Guikema et al. (20) utilized three key variables–census tract population, maximum gust wind speed, and duration of winds above 20 m/s–to estimate outage rates, achieving strong predictive accuracy for most tested storms. McRoberts et al. (41) later enhanced the model's accuracy by implementing a two-stage random forest model, building on the work of Guikema and Quiring (42). The first stage uses a binary random forest classification model to determine whether a census tract will experience power outages. The second stage, conditional to the first stage predicting outages, uses a random forest regression model to estimate the fraction of customers without power in those tracts. This updated model included additional environmental variables such as topography, tree characteristics, land cover, soil moisture, and precipitation.

To adapt the model for estimating outages across 25 states along the Gulf and Atlantic coasts, we excluded variables from the McRoberts et al. (41) model that were unavailable at this geographical scale, such as tree characteristics. The covariates considered in the retraining process included population, land cover, topography, soil moisture, and tropical cyclone wind data. The population density data were obtained from the US Census Bureau. The land cover data, obtained from the Land Cover Database, included eight land use classifications: water, developed, barren, forest, shrubland, herbaceous, planted/cultivated, and wetlands. The topography data–mean, median, SD, minimum, and maximum elevation–were obtained from the digital elevation model (DEM) produced by the US Geological Survey. The soil moisture data, obtained from North America Land Data Assimilation System Phase 2 (NLDAS-2), includes measurements at three levels: 0 to 10 cm, 10 to 40 cm, and 40 to 100 cm. Finally, the tropical cyclone wind data include the maximum surface-level (10 m) gust wind speed over the length of the tropical cyclone at the center of the census tract and the duration of sustained winds exceeding 20 m/s.

For validation, we used holdout cross-validation with mean absolute error as the performance metric, splitting the outage data into 80% for training and 20% for testing across 30 iterations. The retrained model minimized prediction error with the chosen subset of variables, achieving effective performance across the multistate region. The Mean Absolute Error results indicated that the best performance model, which minimized the prediction error, included population density, land cover variables (forest, herbaceous, and wetlands), maximum surface-level (10 m) gust wind speed, and the duration of sustained winds above 20 m per second. Additional details on the parameter selection process are provided in the Supporting Information.

3.2.2. Power outage simulation. We estimated the fraction of the customers in each census tract that will experience power outages for each tropical cyclone using the two-step regression model with the reduced set of covariates. This analysis estimated the impact of 4,000 tropical cyclones for each GCM, which included 2,000 cyclones for the hindcast period (1985–2014) and 2,000 cyclones for the late-century period (2071–2100).

To estimate the mean fraction of outages per census tract for each GCM and period, we used a Poisson distribution, setting the rate parameter (λ) equal to the annual frequency parameter obtained from the Synthetic Tropical Cyclone Generator. This parameter represents the expected annual frequency of tropical cyclones over a 30-y period. For each Monte Carlo simulation iteration, the Poisson distribution provided the number of cyclones expected for that year. Based on this result, we randomly selected an equivalent number of events from the dataset of tropical cyclones.

Each event in the dataset had an equal probability of selection, as the dataset already incorporates the tropical cyclone intensity distribution. This assumption ensures that the randomly selected hazards appropriately reflect the original hazard intensity distribution for a given year. For each iteration, we recorded the maximum fraction of power outages observed in each census tract, which reflects the worst-case scenario for that year. This approach captures the upper bound of outage impacts across the modeled events. The process was repeated 1,000 times using Monte Carlo simulation techniques to ensure robust statistical sampling.

Upon completing the simulations, we calculated the mean fraction of outages over the 30 y for each GCM. These results enabled us to evaluate and compare the projected impacts of tropical cyclones on the frequency and intensity of power outages at the census tract level along the Gulf and Atlantic Coasts of the United States across both the hindcast and late-century periods. We then calculated the difference in mean fractional outages between the two time periods for each GCM, where positive values indicate a projected increase in the proportion of customers experiencing power outages under 3 °C of warming, and negative values indicate a projected decrease. By estimating these parameters at the census tract level across all GCMs, we captured the variability and uncertainty in tropical cyclone occurrence and its impacts on regional power infrastructure under different climate scenarios.

To address the uncertainties in climate model projections, we evaluated the level of agreement (AL) across the seven GCMs. This approach enabled us to identify areas of consensus, where projections from multiple models align, and areas of disagreement, which highlight potential uncertainties. Agreement is defined as cases where at least 5 out of 7 models concur on the outage projection trend–either an increase or decrease–while all other cases are categorized as disagreement.

3.2.3. Power outage restoration. Understanding restoration times is essential to capture the full impact of increases in both the number and duration of outages, particularly as they contribute to the economic impacts discussed in the following section. However, estimating restoration times on a national scale is challenging due to variations across utilities, which depend on factors such as crew management practices and real-time operational decisions. Given these complexities, we use a straightforward estimation approach with the aim of refining it in future research.

For this analysis, we utilize outage duration data, in minutes, per Saffir–Simpson categories, calculated using outage data from poweroutages.us, a website that scrapes outage data from utilities. These estimates are based on a statistical outage duration model trained on tropical cyclones from 2013 to 2020. Using central estimates of outage duration, we developed a piecewise linear relationship between outage minutes and the wind speed range associated with each category.

To estimate event frequency, we assume the occurrences follow a Poisson distribution, where the median point is calculated as $1/e^{v}$, with v representing the maximum wind speed at landfall. Due to this simplified approach, all customers are assigned the same outage duration for a given event.

3.3. Distributional Impact Model.

For our distributional impact analysis, we evaluated the relationship between sociodemographic and socioeconomic variables, including the Social Vulnerability Index (SVI), and tropical cyclone–induced power outage risks. The selected variables included sociodemographic factors such as the proportions of females, children, elderly individuals, White and Hispanic populations, and individuals with disabilities, as well as socioeconomic factors like populations with education below the high school level, poverty levels, and median household income. Additionally, we included the Social Vulnerability Index (SVI), a composite measure that incorporates multiple factors contributing to social vulnerability.

Sociodemographic data, including gender, race, ethnicity, age, and education, were obtained from the 2020 Decennial Census, while employment and disability rates were obtained from the 2021 American Community Survey (ACS). Socioeconomic data, including median household income and poverty rates, were also sourced from the 2021 ACS. The Social Vulnerability Index was obtained from the 2020 CDC SVI Documentation, which provided a composite measure of vulnerability factors. Additional details on these data sources are included in the Supporting Information (*SI Appendix*, Table S1).

To ensure the robustness of the analysis and minimize multicollinearity, we evaluated all sociodemographic and socioeconomic variables for independence. Variables with a correlation coefficient greater than 40% were considered highly correlated and excluded from the final analysis. For example, median household income and poverty levels exhibited a strong inverse correlation, as areas with higher median income typically had lower poverty levels. By excluding one variable from each highly correlated pair, we retained a final set of variables that allowed for a clearer interpretation of their independent contributions to power outage risks.

To evaluate the relationship between these variables and power outage risks, we implemented a Random Forest regression model, using the "Random Forest" package in R (43). The response variable was the mean fraction of outages for each GCM and period. The explanatory variables consisted of the final set of sociodemographic and socioeconomic variables as well as the SVI.

Then, we utilized the methodology described by Shortridge and Guikema (31) to calculate the total change in the marginal effect of each predictor on the response variable from its Partial Dependence Plots (PDPs). This total change, referred to as the "swing," captures the variability in the predictor's influence on outage risks. The swing represents the difference between the minimum and maximum values of a predictor's PDP. This metric provides insight into both the magnitude and direction of the variable's impact on outage risks. The magnitude of the swing indicates the sensitivity of each variable to power outage risks, with larger swings indicating a greater likelihood of outage impact for the associated subgroup. A positive swing suggests that census tracts with higher concentrations of the subgroup represented by the variable are more likely to experience greater outage risks. Conversely, a negative swing indicates that higher concentrations of that group are associated with reduced outage risks.

It is worth noting that all sociodemographic and socioeconomic variables were held constant between the hindcast and late-century periods. As such, the observed changes in outage risks across these periods reflect only the influence of climate-driven changes in tropical cyclone characteristics. This approach ensures that any changes are attributed only to climate-related factors, without interference from assumptions about future changes in human systems. In other words, it does not account for future demographic, economic, or infrastructural shifts. Future work could incorporate migration and dynamic socioeconomic projections to assess how changing human systems may interact with climate impacts to shape future risk landscapes.

3.4. Economic Model. To estimate the economic impact of these outages, we used the ICE Calculator, which estimates customer interruption costs (CIC) through a two-stage regression model. The first stage uses a probit model that estimates the probability that a customer reports any financial cost from a power interruption, as opposed to reporting no cost at all. This estimate is based on independent variables that capture customer and interruption characteristics. The second stage uses a generalized linear model to relate actual interruption costs for those customers who report financial costs from power interruptions to the set of independent variables (28).

Through these regression models and data from 34 existing CIC studies (27), the ICE Calculator estimates outage costs using several key input variables. These inputs include reliability index values for the System Average Interruption Duration Index (SAIDI), System Average Interruption Frequency Index (SAIFI), and Customer Average Interruption Duration Index (CAIDI), the geographical area affected by outages; the number of residential, commercial, and industrial customers impacted; annual power consumption by customer sector in megawatt hours (MWh); and median household income for residential customers.

To implement the ICE Calculator into our analysis, we first obtained U.S. utility service territory information from the US Energy Information Administration (EIA) through the Annual Electric Power Industry Report data, collected through the Form EIA-861 survey (44). This form provides historical data from 1990–2021, including reliability indices from 2013 onward, sector-specific customer counts, and annual electricity sales by sector, for each utility service territory impacted by increased tropical cyclone–related power interruptions. The reliability index values compiled were SAIDI, SAIFI, and CAIDI. SAIDI indicates the cumulative annual duration of interruptions for the average customer; SAIFI indicates the average annual number of interruptions for each customer; and CAIDI indicates the average outage length per customer, or the average electricity service restoration time (27).

We extracted the two-stage regression model framework and regional data from the ICE Calculator model available online (45) and reconstructed a functional version in R to enable iterative processing of each modeled tropical cyclone track in our analysis. Using spatial data on the centers of population coordinates for each census tract (46) and a utility service territory shapefile (47), we mapped each census tract to its corresponding utility service area.

For each affected census tract population ((48) and utility service territory, we stored the proportions of residential, commercial, and industrial sector customers (from 2021 data or 2016–2020 average where the former was unavailable), along with their respective MWh sales obtained from the EIA-861 Form, and the adjusted reliability index values based on our projected tropical cyclone interruptions. These inputs, along with the regression models, regional timing of outage (time of day or year), commercial and industrial customer characteristic data for each census-tract iteration were processed in the ICE calculator to estimate the interruption cost per event for each customer. Additional details are provided in the *SI Appendix*, section 5.

We expect an increase in the number of customers over time, which is expected to further increase the impact of power outages. To account for growth, we use population projections for residential customers and recent trends to represent growth in commercial and industrial customers. Consistent with other CIRA sectoral analyses, we use state-level population projections from the Integrated Climate and Land Use Scenarios version 2 (ICLUSv2) model (49, 50) along with the United Nations' (51) Median variant projection, which is based on assumptions of medium levels of fertility, mortality, and migration (52). For commercial and industrial customers, we assume growth follows recent linear trends extracted from the state-level customer data described above (44) for 1990–2021. More details are provided in the Supporting Information (*SI Appendix*, Table S6).

3.5. Uncertainty. We acknowledge that there is substantial uncertainty in any projection this far into the future, uncertainty that arises from many sources. A full uncertainty propagation and quantification is beyond the scope of this paper, and future work could expand on our modeling to more fully account for and propagate uncertainty.

Previous work on projecting hurricane power outage risk into the future suggested that uncertainty in projected hurricane outage rates is dominated by uncertainty in hurricane frequency (8). Starting from this earlier finding, we expanded on the sources of uncertainty considered and focused on the uncertainty in 1) future climate state as represented by uncertainty in the GCMs and 2) uncertainty in hurricane frequency, track, and intensity. We did not include uncertainty in power outages for a given hurricane, in power outage restoration given an outage event, or in the economic impacts. The uncertainty bounds provided in Table 1 thus reflect the uncertainty due to climate models and downscaled hurricanes for each climate model. We acknowledge that this is an incomplete representation of uncertainty, but it captures the dominant source of uncertainty suggested by Alemazkoor et al. (8) and goes beyond this to more fully capture hurricane frequency, location, and track uncertainty as well.

We note that we did not project changes in demographic or economic variables into the future. We are unaware of any study that has done this for projecting power outages into the future. If this were to be done, this would contribute substantial uncertainty to the estimated changes. This is left for future work.

Finally, we note that we did not project changes in the electric power grid into the future. These changes are highly uncertain and depend in part on policies, incentives, and regulations put in place in the coming decades. This makes changes in the electric power grid difficult to project with any degree of confidence. One can imagine that if current grid resilience enhancement programs continue, the electric power grid of the future may experience reduced disruptions due to hurricanes. If this were to occur, future outage rates may be lower than we have estimated.

Data, Materials, and Software Availability. Some of the data used in this research, particularly the detailed hurricane track data, is available only under a non-commercial, non-distributed use agreement. This can be made available from the authors for non-commercial uses but requires a non-disclosure statement to be signed. The data underlying the figures and results in the paper are available publicly (53). The code for the paper also requires a non-disclosure statement.

ACKNOWLEDGMENTS. We would like to thank Peter Larsen from Lawrence Berkley National Laboratory for guidance on the ICE model as well as Robert Harris for the calculating outage duration statistics used to estimate outage durations in his working paper titled, "Willingness to Pay for Electricity Reliability: Evidence from U.S. Generator Sales" from 2023. Components of this work were funded under EPA contract # 68HERH19D0028. The views expressed in this paper are solely those of the authors and do not necessarily represent the views or policies of their employers.

Author affiliations: [a]Civil and Environmental Engineering, University of Michigan, Ann Arbor, MI 48109; [b]Industrial and Operations Engineering, University of Michigan, Ann Arbor, MI 48109; [c]Industrial Economics, Inc, Cambridge, MA 02140; [d]WindRiskTech, L.L.C., New Harbor, ME 04554; and [e]U.S. Environmental Protection Agency, Washington, DC 20460

1. E. Mills, Extreme Grid Disruptions and Extreme Weather, Lawrence Berkeley National Laboratory, U.S. Disaster Reanalysis Workshop, May 3, 2012 (2012) http://evanmills.lbl.gov/presentations/Mills-Grid-Disruptions-NCDC-3May2012.pdf.
2. U.S. Department of Energy, Electric emergency incident and disturbance report: Annual summaries. (OE-417) Washington, D.C. (2015).
3. J. A. Casey, M. Fukurai, D. Hernández, S. Balsari, M. V. Kiang, Power outages and community health: A narrative review. *Curr. Environ. Health Rep.* **7**, 371–383 (2020), 10.1007/s40572-020-00295-0.
4. K. Best *et al.*, Spatial regression identifies socioeconomic inequality in multi-stage power outage recovery after Hurricane Isaac. *Nat. Hazards* **117**, 851–873 (2023), 10.1007/s11069-023-05886-2.
5. R. J. Campbell, Weather-related power outages and electric system resiliency. Congressional research service report for congress. 7-5700 R42696 (2012). www.crs.gov.
6. K. Lacommare, J. Eto, Cost of power interruptions to electricity consumers in the United States (US). *Energy* **31**, 1845–1855 (2006), 10.1016/j.energy.2006.02.008.
7. Primen, The cost of power disturbances to industrial and digital economy companies. Primen. TR-1006274 (Available through EPRI). June 29. Madison WI (2001).
8. N. Alemazkoor *et al.*, Hurricane-induced power outage risk under climate change is primarily driven by the uncertainty in projections of future hurricane frequency. *Sci. Rep.* **10**, 15270 (2020), 10.1038/s41598-020-72207-z.
9. K. Marvel *et al.*, "Climate trends" in *Fifth National Climate Assessment*. A. R. Crimmins *et al.*, Eds. (U.S. Global Change Research Program, Washington, DC, 2023), Ch. 2, 10.7930/NCA5.2023.CH2.
10. Intergovernmental Panel on Climate Change (IPCC), "Weather and Climate Extreme Events in a Changing Climate" in *Climate Change 2021–The Physical Science Basis: Working Group I Contribution to the Sixth Assessment Report of the Intergovernmental Panel on Climate Change* (Cambridge University Press, Cambridge, 2023a) 1513–1766, https://doi.org/10.1017/9781009157896.013.
11. Intergovernmental Panel on Climate Change (IPCC), "Climate Change Information for Regional Impact and for Risk Assessment" in *Climate Change 2021–The Physical Science Basis: Working Group I Contribution to the Sixth Assessment Report of the Intergovernmental Panel on Climate Change* (Cambridge University Press, Cambridge, 2023b), pp. 1767–1926, https://doi.org/10.1017/9781009157896.014.
12. S. Han *et al.*, Estimating the spatial distribution of power outages during hurricanes in the Gulf coast region. *Reliab. Eng. Syst. Saf.* **94**, 199–210 (2009a). 10.1016/j.ress.2008.02.018.
13. S. Han, S. D. Guikema, S. M. Quiring, Improving the predictive accuracy of hurricane power outage forecasts using generalized additive models. *Risk Anal.* **29**, 1443–1453 (2009b), 10.1111/j.1539--6924.2009.01280.x.
14. R. Nateghi, S. Guikema, S. M. Quiring, Power outage estimation for tropical cyclones: Improved accuracy with simpler models. *Risk Anal.* **34**, 1069–1078 (2014), 10.1111/risa.12131.
15. S. M. Quiring, A. B. Schumacher, S. D. Guikema, Incorporating hurricane forecast uncertainty into a decision-support application for power outage modeling. *Bull. Am. Meteor. Soc.* **95**, 47–58 (2014), 10.1175/bams-d-12-00012.1.
16. J. He *et al.*, Nonparametric tree-based predictive modeling of storm outages on an electric distribution network. *Risk Anal.* **37**, 441–458 (2017), 10.1111/risa.12652.
17. S. Shashaani, S. D. Guikema, C. Zhai, J. V. Pino, S. M. Quiring, Multi-stage prediction for zero-inflated hurricane induced power outages. *IEEE Access* **6**, 62432–62449 (2018), 10.1109/access.2018.2877078.
18. W. O. Taylor *et al.*, Machine learning evaluation of storm-related transmission outage factors and risk. *Sustain. Energy Grids Netw.* **34**, 101016 (2023), 10.1016/j.segan.2023.101016.
19. K. Fatima, H. Shareef, F. B. Costa, A. A. Bajwa, L. A. Wong, Machine learning for power outage prediction during hurricanes: An extensive review. *Eng. Appl. Artif. Intell.* **133**, 108056 (2024), 10.1016/j.engappai.2024.108056.
20. S. D. Guikema *et al.*, Predicting hurricane power outages to support storm response planning. *IEEE Access* **2**, 1364–1373 (2014), 10.1109/access.2014.2365716.
21. S. D. Guikema, I. Udoh, J. Irish, R. Nateghi, "The effects of hurricane surge in power system outage risk models" in *Proceedings Probabilistic Safety Assessment Manage* (ESREL, 2012).
22. G. L. Tonn, S. D. Guikema, C. M. Ferreira, S. M. Quiring, Hurricane isaac: A longitudinal analysis of storm characteristics and power outage risk. *Risk Analysis* **36**, 1936–1947 (2016), 10.1111/risa.12552.
23. D. Mitsova, A.-M. Esnard, A. Sapat, B. S. Lai, Socioeconomic vulnerability and electric power restoration timelines in Florida: The case of hurricane Irma. *Nat. Hazards* **94**, 689–709 (2018), 10.1007/s11069-018-3413-x.
24. K. Cox, B. Kim, Race and income disparities in disaster preparedness in old age. *J. Gerontol. Soc. Work* **61**, 719–734 (2018), 10.1080/01634372.2018.1489929.
25. R. S. Liévanos, C. Horne, Unequal resilience: The duration of electricity outages. *Energy Policy* **108**, 201–211 (2017).
26. M. O. Román *et al.*, Satellite-based assessment of electricity restoration efforts in Puerto Rico after Hurricane Maria. *PLoS One* **14**, e0218883 (2019), 10.1371/journal.pone.0218883.
27. M. Sullivan, M. T. Collins, J. Schellenberg, P. H. Larsen, *Estimating Power System Interruption Costs: A Guidebook for Electric Utilities* (Nexant, Inc. and Lawrence Berkeley National Laboratory, 2018).
28. M. Sullivan, J. Schellenberg, M. Blundell, *Updated Value of Service Reliability Estimates for Electric Utility Customers in the United States* (Lawrence Berkeley National Laboratory, Berkeley, 2015).
29. M. C. Sarofim *et al.*, High radiative forcing climate scenario relevance analyzed with a ten-million-member ensemble. *Nat. Commun.* **15**, 8185 (2024), 10.1038/s41467-024-52437-9.
30. T. Knutson, Coauthors, Tropical cyclones and climate change assessment: Part II: Projected response to anthropogenic warming. *Bull. Am. Meteorol. Soc.* **101**, E303–E322 (2020), 10.1175/BAMS-D-18-0194.1.
31. J. E. Shortridge, S. D. Guikema, Public health and pipe breaks in water distribution systems: Analysis with internet search volume as a proxy. *Water Res.* **53**, 26–34 (2014).
32. C. Fant *et al.*, Climate change impacts and costs to U.S. electricity transmission and distribution infrastructure. *Energy* **195**, 116899 (2020), 10.1016/j.energy.2020.116899.
33. K. Emanuel, Climate and tropical cyclone activity: A new model downscaling approach. *J. Climate* **19**, 4797–4802 (2006), 10.1175/jcli3908.1.
34. K. Emanuel, R. Sundararajan, J. Williams, Hurricanes and Global Warming: Results from Downscaling IPCC AR4 Simulations. *Bulletin of the American Meteorological Society* **89**, 347–368 (2008). 10.1175/bams-89-3-347.
35. K. A. Emanuel, Downscaling CMIP5 climate models shows increased tropical cyclone activity over the 21st century. *Proc. Natl. Acad. Sci. U.S.A.* **110**, 12219–12224 (2013), 10.1073/pnas.1301293110.
36. M. Komurcu, K. A. Emanuel, M. Huber, R. P. Acosta, High-resolution climate projections for the Northeastern United States using dynamical downscaling at convection-permitting scales. *Earth Space Sci.* **5**, 801–826 (2018a). 10.1029/2018ea000426.
37. H. Hersbach *et al.*, The ERA5 global reanalysis. *Q. J. R. Meteorol. Soc.* **146**, 1999–2049 (2020), 10.1002/qj.3803.
38. C. Tebaldi, A. Armbruster, H. Engler, R. Link, Emulating climate extreme indices. *Environ. Res. Lett.* **15**, 074006 (2020), 10.1088/1748-9326/ab8332.
39. M. C. Sarofim *et al.*, A temperature binning approach for multi-sector climate impact analysis. *Clim. Change* **165**, 10 .1007/s10584-021-03048-6 (2021). 10.1007/s10584-021-03048-6.
40. H. E. Willoughby, R. W. R. Darling, M. E. Rahn, Parametric representation of the primary hurricane vortex. Part II: A new family of sectionally continuous profiles. *Mon. Weather Rev.* **134**, 1102–1120 (2006), 10.1175/MWR3106.1.
41. D. B. McRoberts, S. M. Quiring, S. D. Guikema, Improving hurricane power outage prediction models through the inclusion of local environmental factors. *Risk Anal.* **38**, 2722–2737 (2018), 10.1111/risa.12728.
42. S. Guikema, S. Quiring, Hybrid data mining-regression for infrastructure risk assessment based on zero-inflated data. *Reliab. Eng. Syst. Saf.* **99**, 178–182 (2011), 10.1016/j.ress.2011.10.012.
43. A. Liaw, M. Wiener, Classification and regression by randomForest. *R News* **2/3**, 18–19 (2002), https://journal.r-project.org/articles/RN-2002-022/RN-2002-022.pdf.
44. U.S. Energy Information Administration (EIA), Annual electric power industry report, Form EIA-861 detailed data files. EIA Electricity (2022). https://www.eia.gov/electricity/data/eia861/.
45. U.S. Department of Energy, Lawrence Berkeley National Laboratory, and Resource Innovations, Inc. (formerly Nexant, Inc.). (2018). Interruption Cost Estimate (ICE) Calculator. ICE Calculator (2018).
46. U. S. Census Bureau, Centers of population. Census reference files (2020), https://www.census.gov/geographies/reference-files/time-series/geo/centers-population.html.
47. U.S. Energy Information Administration (EIA), Electric retail service territories (2022b), https://atlas.eia.gov/datasets/f4cd55044b924fed9bc8b64022966097_0/explore?location=40.633911%2C-73.600022%2C7.00.
48. U. S. Census Bureau, Decennial census redistricting data: Race (2020), https://data.census.gov/table?q=population&g=010XX00US$1400000&tid=DECENNIALPL2020.P1.
49. B. G. Bierwagen *et al.*, National housing and impervious surface scenarios for integrated climate impact assessments. *Proc. Natl. Acad. Sci. U.S.A.* **107**, 20887–20892 (2010a), 10.1073/pnas.1002096107.
50. EPA, Multi-model framework for quantitative sectoral impacts analysis: A technical report for the fourth national climate assessment (U.S. Environmental Protection Agency, EPA 430-R-17-001, 2017).
51. United Nations, Department of Economic and Social Affairs, Population Division. World Population Prospects: The 2015 Revision, Volume I: Comprehensive Tables (ST/ESA/SER.A/379) (2015).
52. B. C. O'Neill *et al.*, A new scenario framework for climate change research: The concept of shared socioeconomic pathways. *Clim. Change* **122**, 387–400 (2013). 10.1007/s10584-013-0905-2.
53. S. Guikema, "Replication data for: Climate change impacts on tropical cyclone-induced power outage risk: Socio-demographic differences in outage burdens." Harvard Dataverse, V1. https://doi.org/10.7910/DVN/0KHAJN.